Enhanced iron magnetic moment in the ThFe11C2 intermetallic compound

D. Benea, O. Isnard, J. Minár, H. Ebert, and V. Pop

Citation: Journal of Applied Physics **109**, 083909 (2011); doi: 10.1063/1.3567923
View online: http://dx.doi.org/10.1063/1.3567923
View Table of Contents: http://scitation.aip.org/content/aip/journal/jap/109/8?ver=pdfcov
Published by the AIP Publishing

Enhanced iron magnetic moment in the $ThFe_{11}C_2$ intermetallic compound

D. Benea,[1,a)] O. Isnard,[2,3] J. Minár,[4] H. Ebert,[4] and V. Pop[1]
[1]*Babes Bolyai University Faculty of Physics, 400084 Cluj-Napoca, Romania*
[2]*Institut Néel, CNRS, Université Joseph Fourier, BP166, 38042 Grenoble cedex, France*
[3]*Institut Universitaire de France, Maison des Universités, 103 Boulevard Saint Michel, 75005 Paris cedex, France*
[4]*Department Chemie, Universität München, Butenandtstr. 5-13, München, D-81377 Germany*

(Received 19 November 2010; accepted 19 February 2011; published online 19 April 2011)

Detailed theoretical investigations on the electronic and magnetic properties of the $ThFe_{11}C_2$ compound have been performed using both the linear muffin-tin orbital and Korringa–Kohn–Rostocker methods of band structure calculation. The structure of the $ThFe_{11}C_2$ compound has three inequivalent iron sites with different local environment. A strongly enhanced magnetic moment is observed on certain Fe positions, coexisting with much lower magnetic moments on other iron positions of the lattice. Band structure calculations indeed show that the Fe magnetic moments depend strongly on the local environment. The average Fe magnetic moment obtained from these calculations is in good agreement with the experimental average Fe moment obtained from magnetization measurements. The orbital contribution to the magnetic moment is found to be especially large on the Fe 4b position. Comparing calculated hyperfine fields with experimental results, it is found that the calculated and experimental hyperfine fields are correlated. However, similarly to the results reported before for elemental Fe, the magnitude of all calculated Fe hyperfine fields is about 25% smaller. The agreement with the Mössbauer measurements is improved by scaling the core polarization contribution and by estimating the orbital valence *d*-electrons contribution to the magnetic hyperfine fields using the local spin density approximation + dynamical mean field theory calculated orbital moments. © *2011 American Institute of Physics*. [doi:10.1063/1.3567923]

I. INTRODUCTION

Intermetallic compounds with 4*f* or 5*f* elements and transition metals exhibit remarkable magnetic properties that enable their use as hard magnets. Also, these compounds are a challenging class of materials, interesting for fundamental research because of their prominent physical properties such as, for example, the magnetic exchange interaction and magnetocrystalline anisotropy.

In the last few years, many investigations have been performed to study the influence of interstitial elements (C, N, or H) on the Curie temperature or the magnetization of Fe-rich materials in binary or ternary compounds. The binary Fe–N and Fe–C compounds also have attracted much interest, particularly $Fe_{16}N_2$, since giant magnetic moments have been found for Fe, thus leading to intensive research on both bulk and thin films samples in the last decades.[1–5] In the meantime, ternary compounds containing rare-earth elements or thorium, transition metals, and metalloids also have been investigated.

Among these newly discovered phases, the $ThFe_{11}C_x$ compounds deriving from $BaCd_{11}$ structure type[6,7] have been evidenced. This carbon stabilized type of interstitial alloy is isotypic with the manganese-based series $LaMn_{11}C_{2-x}$ (Ref. 8) and with the pseudoternary $RFe_{10}SiC_{0.5}$ (R = Ce, Pr, Nd, Sm).[9] For R = Th it was found that no Si substitution was required to stabilize the phase. A structural investigation of the $ThFe_{11}C_x$ phases has been reported elsewhere.[10] The investigations of the magnetic properties of $ThFe_{11}C_{1.5}$ and $ThFe_{11}C_{1.8}$ compounds show that the C concentration has a large effect on all magnetic properties of these compounds.[10,11] The Curie temperature and the Fe–Fe exchange interaction increase with carbon content in the compound. The Curie temperature determined using Arrott plots is 419 K for $ThFe_{11}C_{1.5}$ and 512 K for $ThFe_{11}C_{1.8}$, respectively. On the other hand, the saturation magnetization and the paramagnetic effective moments decrease by increasing the carbon concentration. According to Isnard *et al.*,[11] the spontaneous magnetization at 5 K is 22.0 μ_B and 20.7 μ_B per formula unit for $ThFe_{11}C_{1.5}$ and $ThFe_{11}C_{1.8}$, respectively. The effective Fe moments and the Curie temperature are of the same order of magnitude as in the binary compound Fe_3C (Refs. 12–14) and the 3*d* magnetism is significantly delocalized when compared with α-Fe.[11] A spin reorientation transition takes place at low temperatures, a result of the competition between anisotropy terms of the Fe sublattices.[15,16] In addition, the later studies on $ThFe_{11}C_x$ ($x = 1.5$ and 1.8) show that the spin reorientation temperature decreases significantly upon increasing the pressure.[15]

Linear muffin-tin orbital (LMTO) and spin polarized relativistic Korringa–Kohn–Rostocker (SPR-KKR) band structure calculations have been performed in order to investigate the magnetic properties of the $ThFe_{11}C_2$ compound and to correlate the results with previous experimental measurements.[10,11] Th–Fe–C hybridization effect is investigated and the influence of the local environment on the magnitude of

a)Electronic mail: diana.benea@phys.ubbcluj.ro.

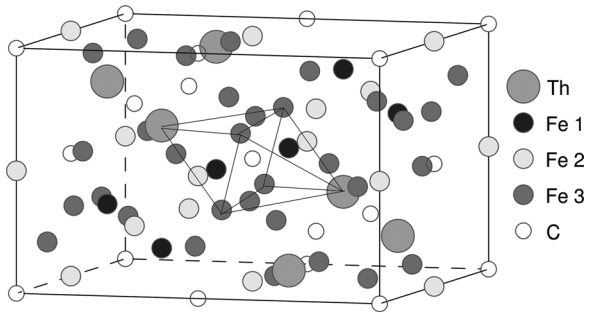

FIG. 1. The crystal structure of the $ThFe_{11}C_x$ compounds.

the Fe magnetic moments and hyperfine fields is discussed. For a more appropriate description of the orbital magnetic properties of the $ThFe_{11}C_2$ compound we used the dynamical mean field theory (DMFT) as implemented within the KKR method.[17] The local spin density approximation + dynamical mean field theory (LSDA + DMFT) calculated orbital magnetic moments have been used to scale the valence band contribution to the hyperfine field of Fe atoms. We also scaled the core polarization contribution, underestimated by the LSDA calculation methods,[37,40] in order to improve the agreement with Mössbauer measurements. The paper is organized as follows. Details of the band structure computations are described in Sec. II, the corresponding results are discussed in comparison with earlier reported experimental results in Sec. III, and the conclusions are summarized in Sec. IV.

II. COMPUTATIONAL DETAILS

LMTO electronic band structure calculations in atomic spheres approximation (ASA) have been done in the framework of LSDA to the density functional theory,[18] including the so-called combined correction terms.[19] The calculations have been done in the relativistic mode, i.e., all relativistic effects have been taken into account, including spin-orbit coupling. The LSDA parametrization for the exchange-correlation energy as suggested by Vosko, Wilk, and Nusair was used.[20] The angular momentum expansion of the basis functions was taken up to $l=3$. The k-space integration was performed using the tetrahedron method[21] on a grid of 280 k points in the irreducible part of the Brillouin zone. From the energy bands and the LMTO eigenvectors total and orbital (l-projected) density of states (DOS) functions were calculated.

The SPR-KKR method in the ASA mode[22–24] has been used in addition to determine the electronic structure and magnetic properties of the $ThFe_{11}C_2$ intermetallic compound. The same LSDA parametrization as for the LMTO calculations was used. For integration over the Brillouin zone, the special points method has been used[25] with a comparable k-points density as for the LMTO calculations. Also, the same Wigner–Seitz (ASA) radii for the atomic spheres approximation have been used for both SPR-KKR and LMTO calculations. Details of the SPR-KKR method, in particular the corresponding calculations of the hyperfine fields, have been described in detail elsewhere.[26–28]

Also, a KKR-based approach to deal with many-body effects using the DMFT has been used in particular to describe the magnetic properties of the $ThFe_{11}C_2$ compound. While the spin magnetic moments are described rather accurately by the LSDA, the orbital magnetic moments are systematically underestimated. As it has been shown before,[29,30] accounting explicitly for local correlations within the LSDA + DMFT approach can improve the description of the orbital magnetic moments substantially. We used the LSDA + DMFT scheme, self-consistent with respect to the self-energy and the charge density, as implemented within the relativistic SPR-KKR formalism.[17] As a DMFT solver the relativistic version of the so-called Spin-Polarized T-Matrix Plus Fluctuation Exchange approximation[31,32] was used. The self-energy within the DMFT is parametrized by the average screened Coulomb interaction U and the Hund exchange interaction J. The J parameter can be calculated directly within the LSDA and is approximately the same for all 3d elements. The parameter U is strongly affected by the metallic screening and it is estimated for the 3d metals between 1 and 3 eV. We used $J_{Fe}=0.9$ eV and $U_{Fe}=2.0$ eV for the Fe atoms throughout our calculations.

III. RESULTS AND DISCUSSIONS

As reported in previous work,[6,7,10] the $ThFe_{11}C_x$ compounds crystallize in the $BaCd_{11}$-type structure having $I4_1/amd$ space group symmetry. The corresponding crystal structure is shown in Fig. 1 with site occupation and the coordinates of the atoms in the $ThFe_{11}C_2$ compound presented in Table I. Three inequivalent Fe sites are found in the $BaCd_{11}$ structure type: Fe(1) on the 4b site, Fe(2) on the 8d site, and Fe(3) on the 32i site. The C atoms are located on the interstitial sites on the axis between two Th atoms, at equal distance from four Fe(3) atoms.[10,33] The Fe(3) atoms sitting on 32i sites have the property to adjust their position to the neighbors without major lattice expansion. This allows the structure to take up C atoms with only minor change in the elastic energy of the lattice, thereby increasing the stability due to the additional C-metal atom bonds. The bond lengths in $ThFe_{11}C_x$ compounds ($x=1.35$ and 2) have

TABLE I. The atomic positions in the $BaCd_{11}$ structure type of $ThFe_{11}C_2$ compound (Ref. 10).

Atom	Site	Coordinates			Near neighbors				ASA radii (a.u.)
Th	4a	0	3/4	1/8	4C	8Fe(3)	2Fe(1)	8Fe(3)	4.19
Fe(1)	4b	0	1/4	3/8	4Fe(2)	8Fe(3)	2Th		3.25
Fe(2)	8d	0	0	1/2	4Fe(3)	4Fe(3)	2Fe(1)		2.99
Fe(3)	32i	0.1283	0.0463	0.1935	1C	2Fe(2)	7Fe(3)	Fe(1)	2.35
C	8c	0	0	0	4Fe(3)	2Th	4Fe(3)	2Fe(2)	2.05

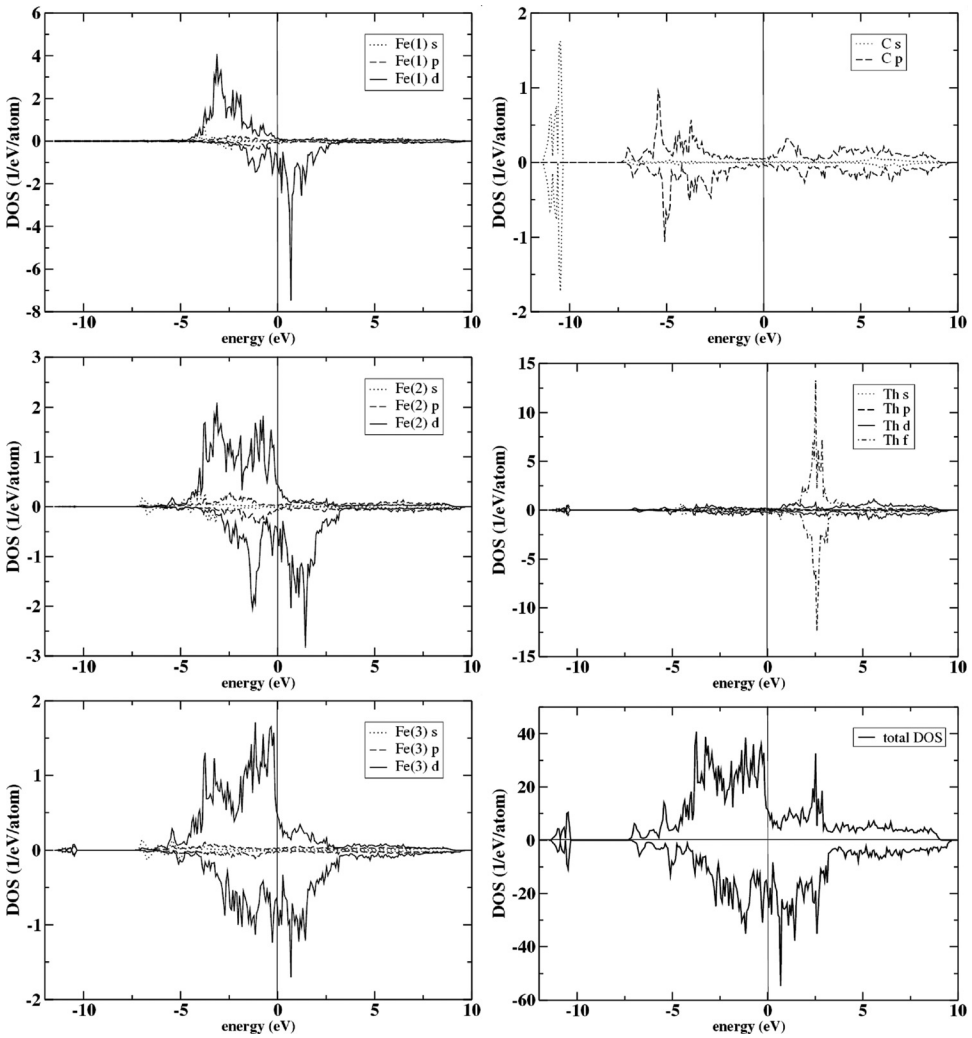

FIG. 2. Spin and component resolved density of states of the $ThFe_{11}C_2$ compound as calculated by the LMTO method.

been determined by Isnard *et al.*[10] The shortest bond length between C and Fe atoms is 1.90 Å for the Fe(3)–C bond in $ThFe_{11}C_2$ compound at 5 K. Also, the Fe–Fe distances within the polyhedron around the C atoms range between 2.53 and 2.75 Å at 5 K for the $ThFe_{11}C_2$ compound.

Relativistic LMTO band structure calculations have been performed for the $ThFe_{11}C_2$ compound in the $BaCd_{11}$ type of structure with the experimental lattice parameters ($a = 10.262$ Å and $c = 6.656$ Å).[10] The Wigner–Seitz (ASA) radii used for the LMTO calculations are shown in Table I. The spin resolved DOS for this compound is presented in Fig. 2. The electronic density of states in the region between −8 eV and the top of the valence band originate from all components with the main contribution stemming from Fe-*d* and C-*p* states. This result reflects the covalent nature of the interatomic bands in $ThFe_{11}C_2$ compound. The Th contribution in the valence band is small; the Th-*f* states are mainly located at the bottom of the conduction band. Near the top of the valence band the contributions of the Fe atoms dominate with smaller contributions from other atoms. As can be seen in Fig. 2, the DOS of the three Fe sites are different in shape. In particular, the Fe(3) sites show a large broadening due to the higher degree of hybridization with their next neighbors, the C atoms which are located at the shortest distance from the Fe(3) atoms (1.90 Å). The observed difference in the exchange-splitting of the three Fe sites reflects the different magnetic moments on the Fe sites. The presence of C interstitial atoms causes charge transfer from C and Th to the Fe(3) atoms partly filling their 3*d* bands and reducing their magnetic moments, as will be shown in the following. It is worth noting that whereas the Fe(2) and Fe(3) atoms are characterized by weak ferromagnetism with none of the 3*d* subbands being completely full, the Fe(1) atom at the 4a position exhibits a strong ferromagnetic behavior with a fully filled 3*d* spin up band. This feature is not very common since iron compounds are often expected to be weak ferromagnet. This enhanced Fe magnetic moment value calculated on the Fe(1) position is significantly larger than the magnetic moment expected from the Slater–Pauling curve whose expected maximum is located at ~2.5 μ_B/atom. This obviously indicates the large effect of the local atomic environment on the magnitude of the Fe magnetic moments.

Neutron diffraction studies,[10] as well as magnetic ordering temperature measurements using a Faraday torque balance,[15] showed that below 200 K the magnetization of the $ThFe_{11}C_{1.8}$ compound is oriented perpendicular to the *c* axis.

TABLE II. The magnetic moments (in μ_B) in the $ThFe_{11}C_2$ compound from LMTO and SPR-KKR calculations on the basis of the LSDA and LSDA + DMFT, respectively.

		Th	Fe(1)	Fe(2)	Fe(3)	C	Total/f.u.
LMTO (LSDA)	m_s	− 0.35	3.25	2.36	1.42	− 0.13	
$M \parallel c$	m_l	0.02	0.12	0.08	0.07	0.00	
	$m_s + m_l$	− 0.33	3.37	2.44	1.49	− 0.13	19.60
LMTO (LSDA)	m_s	− 0.35	3.20	2.35	1.45	–0.15	
$M \perp c$	m_l	0.03	0.10	0.07	0.05	0.00	
	$m_s + m_l$	− 0.32	3.30	2.42	1.50	− 0.15	19.56
SPR-KKR (LSDA)	m_s	− 0.41	3.32	2.57	1.47	− 0.12	
$M \parallel c$	m_l	0.02	0.09	0.06	0.06	0.00	
	$m_s + m_l$	− 0.39	3.41	2.63	1.53	− 0.12	20.30
SPR-KKR (LSDA + DMFT)	m_s	− 0.37	3.36	2.58	1.44	− 0.11	
$M \parallel c$	m_l	0.02	0.15	0.10	0.12	0.00	
	$m_s + m_l$	− 0.35	3.51	2.68	1.56	− 0.11	20.78

The magnetic moments obtained from LMTO band structure calculations for $ThFe_{11}C_2$ with the magnetization perpendicular to the c axis are presented in Table II, together with the magnetic moments calculated by LMTO and SPR-KKR with the magnetization parallel to the c axis.

As one can see in Table II, the band structure calculations indeed show that the Fe magnetic moments strongly depend on the local environment. Small induced magnetic moments are present on Th and C atoms. We note the very good agreement between LMTO and SPR-KKR calculated magnetic moments. An exception occurs for the Fe(2) magnetic moment where the magnitude obtained by these calculation methods differs by about 10%. Both LMTO and SPR-KKR calculation methods show that the highest magnetic moment is that of the Fe(1) atom, which is the most distant atom from C and has the largest distance to the next neighbors (2.70 Å).[10] The smallest magnetic moment occurs for the Fe(3) atom having the metalloid C as nearest neighbors, at 1.90 Å. As the distances to the next neighbors of the Fe atoms are increasing, the hybridization is reduced, favoring the higher magnetic moments for the Fe(2) and Fe(1) atoms. On the Fe(2) position, the LMTO calculated magnetic moment is close to that observed in many iron alloys and compounds including elemental α iron. The large magnetic moment calculated on the Fe(1) position in $ThFe_{11}C_2$ surpasses the largest magnetic moment calculated for $Fe_{16}N_2$.[3,4,34] As expected, the Fe magnetic moments mainly originate from spin, the orbital moments of Fe obtained by the LMTO calculations range between 0.05 and 0.12 μ_B. The orbital moments of Fe are substantially increased when using the LSDA + DMFT calculations compared to the LSDA-based results. It is worth remarking that the orbital magnetic moment of Fe is rather similar on both Fe(2) and (3) sites but is clearly highest for the Fe(1) position. This large orbital moment originates from the peculiar atomic environment made of 14 near neighbors and the presence of a major ligand line.[16] Indeed, such an anisotropic environment is expected to favor the occurrence of an unquenched orbital magnetic moment.

The influence of the local atomic environment on the magnitude of the Fe magnetic moment has been discussed elsewhere[16] and analyzed in terms of: (i) number and type of near neighbors and the type of local symmetry, (ii) the atomic volume of the Wigner–Seitz cell, and (iii) the occurrence of bonds with metalloid near neighbors (B, C, N, …). The hierarchy of the magnetic moments magnitude reported here is in agreement with this analysis.

The average LMTO calculated magnetic moment of Fe in $ThFe_{11}C_2$ is 1.83 μ_B (for $M \perp c$ as well as $M \parallel c$), while the average Fe magnetic moment of $ThFe_{11}C_2$ by SPR-KKR (LSDA) is 1.90 μ_B, in very good agreement with the value of 1.88 μ_B determined from magnetic measurements for the $ThFe_{11}C_{1.8}$ compound.[11] Also, the saturation of magnetization of 20.7 μ_B/f.u. for $ThFe_{11}C_{1.8}$ (Refs. 10 and 11) is in good agreement with the calculated total magnetic moment per formula unit (19.6 μ_B/f.u. from LMTO calculations, 20.3 μ_B/f.u. from SPR-KKR (LSDA) calculations, and 20.78 μ_B/f.u. from SPR-KKR (LSDA + DMFT) calculations, respectively) for $ThFe_{11}C_2$.

The pressure effects on the magnetization of $ThFe_{11}C_{1.5}$ and $ThFe_{11}C_{1.8}$ have been investigated by measurements at low temperatures.[15] The decrease of magnetization with pressure at 5 K is quite low in both samples. The values obtained for $ThFe_{11}C_{1.5}$ and $ThFe_{11}C_{1.8}$ are $d \ln M_s/dP = -1.3 \times 10^{-3}$ kbar^{-1} and $d \ln M_s/dP = -0.3 \times 10^{-3}$ kbar^{-1}, respectively. The LMTO calculations for $ThFe_{11}C_2$ indicate that a hydrostatic pressure of 8.5 kbar would produce a strongly reduced decrease of the total magnetic moment of the system ($m_s + m_l = 19.45$ μ_B/f.u.). This corresponds to a value of $d \ln M_s/dP = -0.6 \times 10^{-3}$ kbar^{-1} comparable with experimental measurements.

The hyperfine fields calculated using the SPR-KKR formalism[28] are presented in Table III together with the results of corresponding Mössbauer measurements.[35] The theoretical hyperfine fields are split into contributions from the core s electrons via Fermi-contact interaction, contribution from non-s core electrons and valence electrons contribution. The non-s electronic contributions are induced by the spin-orbit coupling and they are in general opposite to the normally dominating core polarization field. For Fe the mechanism is connected to the d valence electrons. We notice that the site Fe(3) has the lowest hyperfine field, due to the core

TABLE III. The magnetic hyperfine fields (in kG) in the $ThFe_{11}C_2$ compound.

	Fe(1)	Fe(2)	Fe(3)
Core (*s*)	−376.51	−285.35	−157.81
Core (non-*s*)	1.40	1.17	0.42
Valence	88.99	34.61	−24.58
Valence + core	−286.12	−249.68	−180.87
Estimation[a]	−352	−301	−202
Experiment	−334	−316	−242

[a]Core (*s*) contribution is increased by 25% and valence contribution of *d* electrons is scaled with the ratio l_z^{DMFT}/l_z^{LSDA}, according to Refs. 26 and 37.

contribution, which is about half of the magnitude on other Fe sites. In addition, the valence contribution for this site has the same sign as core contribution to hyperfine field, in contrast to the other sites. The sum (core + valence) is about 60 kG lower than the experimental value for the site Fe(3). The same discrepancies between the calculated hyperfine fields and the values obtained from Mössbauer spectroscopy analysis[35] are present also for Fe(1) and Fe(2) sites. Discrepancies similar to these have been found before for many other systems and have been ascribed to problems dealing with the core polarization contribution when the spin density functional theory is used on a LSDA level.[36–39] In particular, Novák and co-workers[37,40] showed that the contact hyperfine fields for 3*d* transition metal ferromagnets Fe, Co, Ni and some Fe compounds are underestimated by about 20%–30% by LSDA. Also, there are other aspects that have not been accounted for in a satisfactory way by LSDA-based calculations. The orbital contribution at the hyperfine field, which is proportional to the orbital magnetic moment, is also underestimated, as can be seen in Table II by comparing the orbital magnetic moments from SPR-KKR and LSDA + DMFT calculations. In order to account for these defects, we estimated the enhanced hyperfine fields by increasing the core contribution by 25% and scaling the orbital valence contribution of the *d* electrons by the ratio l_z^{DMFT}/l_z^{LSDA}. As can be seen in Table III, this estimation improves the agreement with experiment considerably. Despite the remaining discrepancies related to the hyperfine fields magnitude, we can conclude that the calculated hyperfine field are in qualitative agreement with the measurements and reproduce the site-dependency quite well.

IV. CONCLUSIONS

The investigations of the electronic and magnetic properties of the compound $ThFe_{11}C_2$ revealed differences in the band broadening, exchange splitting, and density of states at the Fermi level for the various Fe sites, leading to rather different magnetic moments for the inequivalent Fe atoms and hybridization with their C, Th, and Fe neighbors. The Fe magnetic moments increase with the increase of the bond lengths between Fe and their next neighbors. More detailed neutron diffraction measurements would be necessary for comparison but the hierarchy of the Fe magnetic moments obtained from the present calculations is in good agreement with the earlier results from Fe Mössbauer spectroscopy.[35] A large difference in the Fe magnetic moment magnitude similar to that revealed by the present calculations on $ThFe_{11}C_2$ has also been reported for binary Fe_5C_2 Hägg carbide.[13] However, in contrast to the binary phase $ThFe_{11}C_2$ exhibits an unusually large magnetic moment on the Fe(1) position of about 3.30 μ_B (for $M \perp c$). This value is significantly larger than the magnetic moment expected from the Slater–Pauling curve. The average Fe magnetic moment and the calculated total magnetic moment per formula unit obtained from LMTO and SPR-KKR calculations are in good agreement with the corresponding values obtained from measurements.[11,15] The hyperfine fields calculated using SPR-KKR band structure method are in qualitative agreement with the values obtained from Mössbauer measurements.[35] However, similar to other previous calculations for Fe,[28,39] the magnitudes of the calculated hyperfine fields are too small. The underestimated LSDA-based contribution of the core electrons has been scaled and the LSDA + DMFT method has been used to improve the valence *d* electrons contribution to the magnetic hyperfine field of Fe atoms, in order to get this way satisfying agreement with results from Mössbauer measurements.

ACKNOWLEDGMENTS

D.B. acknowledges the DAAD support to scientific exchange. This work was partly supported by the Romanian Ministry of Education and Research, Grant No. PNCD II 72-186/2008. J.M. and H.E. acknowledge the financial support of DFG through FOR1346 and Mi-1327/1 projects. V.P. and O.I. warmly acknowledge A. Postnikov for interesting discussions. Also, D.B. would like to acknowledge A. Perlov and A. Yaresko for making available the PY-LMTO package.

[1]Y. Sugita, K. Mitsuoka, M. Komuro, H. Hoshiya, Y. Kozono, and M. Hanazono, J. Appl. Phys. **70**, 5977 (1991).
[2]J. M. D. Coey, J. Appl. Phys. **76**, 6632 (1994).
[3]Y. Sugita, Y. Takahashi, M. Komuro, K. Mitsuoka, and A. Sakuma, J. Appl. Phys. **76**, 6637 (1994).
[4]J. Sakuma, J. Appl. Phys. **79**, 5570 (1996).
[5]K. H. Jack, J. Alloys Compd. **222**, 160 (1995).
[6]T. H. Jacobs, G. L. Long, A. O. Pringle, F. Grandjean, and K. H. J. Buschow, J. Appl. Phys. **70**, 5983 (1991).
[7]T. H. Jacobs, Ph.D. thesis, University of Leiden (1992).
[8]G. Bloch and W. Jeitschko, J. Solid State Chem. **70**, 271 (1987).
[9]J. L. Roy, J. M. Moreau, C. Bertrand, and M. A. Freny, J. Less-Common Met. **136**, 19 (1987).
[10]O. Isnard, J. L. Soubeyroux, D. Fruchart, T. H. Jacobs, and K. H. J. Buschow, J. Phys.: Condens. Matter **4**, 6367 (1992).
[11]O. Isnard, V. Pop, and K. H. J. Buschow, J. Magn. Magn. Mater. **256**, 133 (2003).
[12]M. Ron and Z. Malthalone, Phys. Rev. B **4**, 774 (1971).
[13]G. LeCaer, J. M. Dubois, and J. P. Senateur, J. Solid State Chem. **19**, 19 (1976).
[14]D. Fruchart, P. Chaudouet, R. Fruchart, A. Rouault, and J. P. Senateur, J. Solid State Chem. **51**, 246 (1984).
[15]O. Isnard, Z. Arnold, J. Kamarad, and K. H. J. Buschow, J. Appl. Phys. **99**, 043909 (2006).
[16]O. Isnard and D. Fruchart, J. Alloys Compd. **205**, 1 (1994).
[17]J. Minár, L. Chioncel, A. Perlov, H. Ebert, M. I. Katsnelson, and A. I. Lichtenstein, Phys. Rev. B **72**, 045125 (2005).
[18]U. vonBarth and L. Hedin, J. Phys. C: Solid State Phys. **5**, 1629 (1972).
[19]O. K. Andersen, Phys. Rev. B **12**, 3060 (1975).

[20]S. H. Vosko, L. Wilk, and M. Nusair, Can. J. Phys. **58**, 1200 (1980).
[21]P. E. Blöchl, O. Jepsen, and O. K. Andersen, Phys. Rev. B **49**, 16223 (1994).
[22]P. Weinberger, *Electron Scattering Theory for Order and Disordered Matter* (Oxford University Press, Oxford, 1990).
[23]A. Gonis, *Green Function for Ordered and Disordered Systems* (North-Holland, Amsterdam, 1992).
[24]P. Strange, *Relativistic Quantum Mechanics* (Cambridge University Press, Cambridge, 1998).
[25]H. J. Monkhorst and J. D. Pack, Phys. Rev. B **13**, 5188 (1976).
[26]H. Ebert, in *Electronic Structure and Physical Properties of Solids*, edited by H. Dreyssé (Springer, Berlin, 2000), Vol. 535, p. 191.
[27]H. Ebert, http://olymp.cup.uni-muenchen.de/ak/ebert/sprkkr, The Munich SPRKKR package, version 3.6 (2005).
[28]M. Battocletti and H. Ebert, Phys. Rev. B **64**, 094417 (2001).
[29]S. Chadov, J. Minár, M. I. Katsnelson, H. Ebert, D. Ködderitzsch, and A. I. Lichtenstein, Europhys. Lett. **82**, 37001 (2008).
[30]O. Šipr, J. Minár, S. Mankovsky, and H. Ebert, Phys. Rev. B **78**, 144403 (2008).
[31]M. I. Katsnelson and A. I. Lichtenstein, Eur. Phys. J. B **30**, 9 (2002).
[32]L. V. Pourovskii, M. I. Katsnelson, and A. I. Lichtenstein, Phys. Rev. B **72**, 115106 (2005).
[33]W. B. Pearson, Z. Kristallogr. **152**, 23 (1980).
[34]K. Miura, S. Imanaga, and Y. Hayafuji, J. Phys.: Condens. Matter **5**, 9393 (1993).
[35]G. LeCaer, B. Malaman, O. Isnard, J. L. Soubeyroux, D. Frouchart, T. H. Jacobs, and K. H. J. Buschow, Hyperfine Interact. **77**, 221 (1993).
[36]R. Coehoorn, J. Magn. Magn. Mater. **159**, 55 (1996).
[37]P. Novák, J. Kunes, W. E. Pickett, W. Ku, and F. R. Wagner, Phys. Rev. B **67**, 140403 (2003).
[38]H. Ebert, P. Strange, and B. L. Gyorffy, J. Phys. F: Met. Phys. **18**, L135 (1988).
[39]H. Ebert and H. Akai, Hyperfine Interact. **78**, 361 (1993).
[40]P. Novák and V. Chlan, Phys. Rev. B **81**, 174412 (2010).